ISBN: 978-3-95450-227-1 ISSN: 2673-5490 doi:10.18429/JACoW-IPAC2022-THPOMS004

ACHROMATIC GANTRY DESIGN USING FIXED-FIELD SPIRAL COMBINED-FUNCTION MAGNETS

R. Tesse*, C. Hernalsteens[1], E. Gnacadja, E. Ramoisiaux, N. Pauly, M. Vanwelde
Université libre de Bruxelles, Brussels, Belgium
[1] also at CERN, Geneva, Switzerland

Abstract

Arc-therapy and flash therapy are promising proton therapy treatment modalities as they enable further sparing of the healthy tissues surrounding the tumor site. They impose strong constraints on the beam delivery system and rotating gantry structure, in particular in providing high dose rate and fast energy scanning. Fixed-field achromatic transport lattices potentially satisfy both constraints in allowing instant energy modulation and sufficient transmission efficiency while providing a compact footprint. The presented design study uses fixed-field magnets with spiral edges respecting the FFA scaling law. The cell structure and the layout are studied in simulation and integrated in a compact gantry. Results and further optimizations are discussed.

INTRODUCTION

The treatment of cancer is a major societal challenge for which numerous treatment techniques are actively developed. Novel proton therapy treatment modalities, such as flash and arc therapy, aim at increasing the clinical efficiency and reducing the treatment time. These techniques pose new challenges for the accelerators and beam delivery systems as they require tighter control of the beam spot sizes at the isocenter, better control of beam losses and higher beam currents [1–3]. Gantry designs providing achromatic transport with fixed-field magnets meet these challenges and allow arbitrarily fast energy scanning. We report on a preliminary design of the CASPRO ("Compact Achromatic System for Proton Therapy") project, for an achromatic proton gantry in the energy range 70-230 MeV using normal conducting magnets. The objective is to retain the reduced footprint of modern variable-field compact gantries, such as the IBA Proteus One [4] or the ProNova SC360 superconducting gantry [5]. The adopted strategy is to divide the system into three distinct blocks. The proposed block diagram, presented in Fig. 1, is as follows. A proton beam with an energy of 230 MeV enters the first block that consists of a fixed dipole that deflects the beam and is sent on an energy degrader mounted directly on the gantry, to make the system more compact. The beam transport line following the degrader follows a straight scaling fixed-field lattice design. The second block, detailed in this paper, bends the beam towards the isocenter and is at the heart of the design to reduce the footprint by providing a small bending radius and achromatic properties across the entire energy range. The studied concept is based on Fixed-Field Alternating Gradient (FFAGs) cells using normal conducting magnets. The starting point is the spiral FFAG cells of the RACCAM design [6–9]. The third block is composed of the scanning magnets that are positioned downstream of the last cell to limit the opening of the FFA magnets.

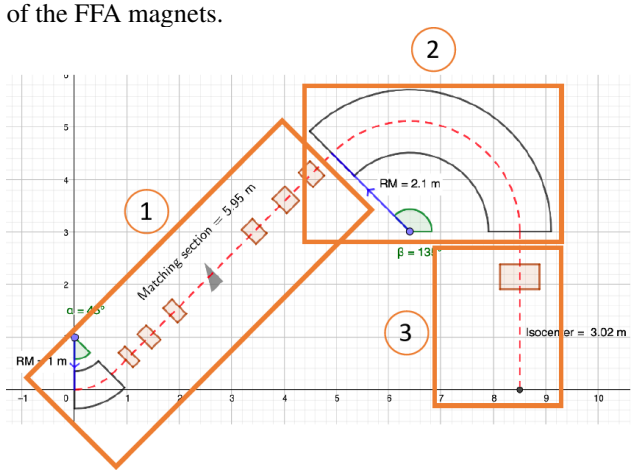

Figure 1: The proposed structure for the CASPRO achromatic gantry. The three main blocks are highlighted in orange.

SPIRAL FFA CELL

We adapt the design of the RACCAM original cell aiming to minimize the size of the magnets. The parameters before and after optimisation are presented in Table 1. An additional constraint arise from the the fact the gantry design uses downstream scanning magnets to scan the beam at isocenter. To minimize the required in-plane aperture of the scanning magnets, the orbit excursion with energy has to be minized. The aim is to keep the excursion span over the full energy range below 20 cm.

Table 1: Periodic Cell Parameters of the RACCAM Design and the Preliminary Design of the Gantry Cell

Parameters (units)	RACCAM	CASPRO
Mean radius R_0 (m)	3.48	2.1
Angle (degrees)	45	45
Field index	4.415	6.0
Spiral angle (degrees)	50.36	65
Field at R_0 (T)	1.5	1.6
Gap (cm)	3	3

The simulations are performed with the ray-tracing code Zgoubi [10, 11] using the Zgoubidoo Python interface [12]. Zgoubidoo provides many additionnal functionalities, such

* robin.tesse@ulb.be

ISBN: 978-3-95450-227-1 ISSN: 2673-5490 doi:10.18429/JACoW-IPAC2022-THPOMS004

as such the ability of running multiple instances of Zgoubi for parallel tracking, analyzing tracking results, and plotting the beamline geometry in a global coordinates system with particle trajectories. With these different modules, Zgoubidoo is suited to study non-linear accelerators such as FFAs [13]. Figure 2 shows the reduction in footprint after modifications of the original cell.

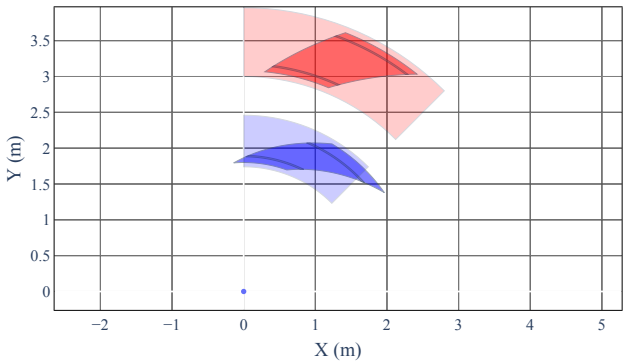

Figure 2: Footprint comparison between the RACCAM cell (in red) and the gantry cell (in blue). We observe the reduction of the footprint with respect to the original design.

First, we determine the periodic closed-orbit solutions for the cell in the energy range 70-230 MeV. The results are shown in Figs. 3 and 4. The periodic trajectory solution, visible in Fig. 3, indicate that a solution is found over the full energy range and that the constraint on excursion is satisfied. The positions and angles as a function of the energy are shown in Fig. 4. It is also essential to ensure that the system

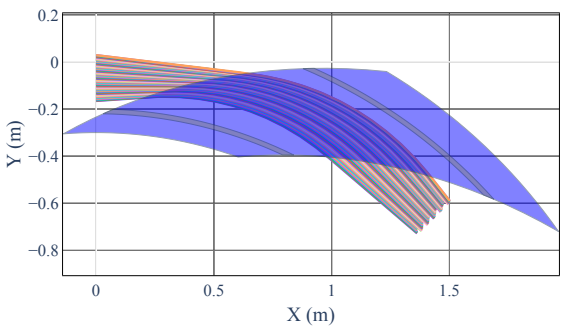

Figure 3: Representation of the cell in a global coordinate system and periodic closed-orbits in the energy range 70-230 MeV. The geometry of the magnet is shown in blue. One clearly see the edge of the magnet which has a spiral curvature and the beam pipe in gray.

can remain normal-conducting. For this purpose, we analyze the field along the particle trajectory at different energies in a cell. As we observe in Fig. 5, the field remains well below 2.3 T. The next study concerns the computation of the Twiss parameters with the beta functions. In Fig. 6, the evolution of the beta function inside the FFA cell is shown, and we observe the periodicity of these functions. The initial beta values for both planes at the cell's entrance as a function of the momentum deviation are shown in Fig. 7.

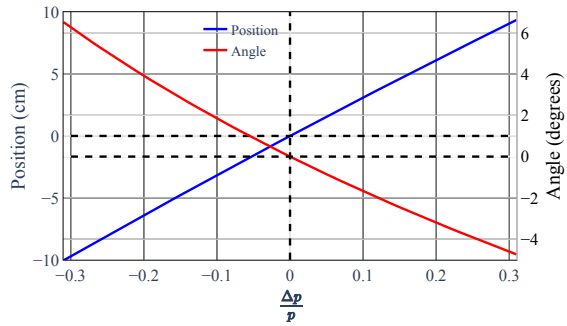

Figure 4: Position (in blue) and angle (in red) of the stable orbit as a function of the momentum deviation at the cell entrance.

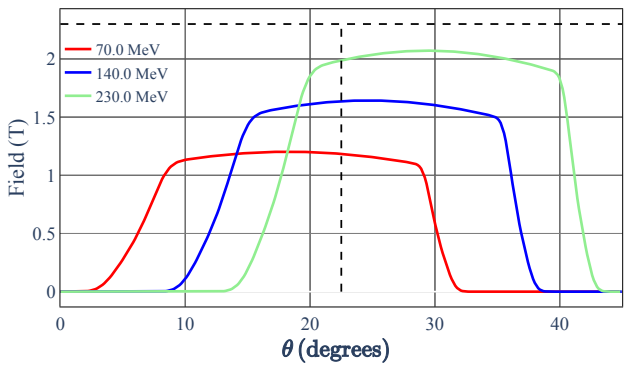

Figure 5: Magnetic field along the particle trajectory at different energies in a cell. For all trajectory, the field is below 2.3 T which ensure normal-conducting magnets.

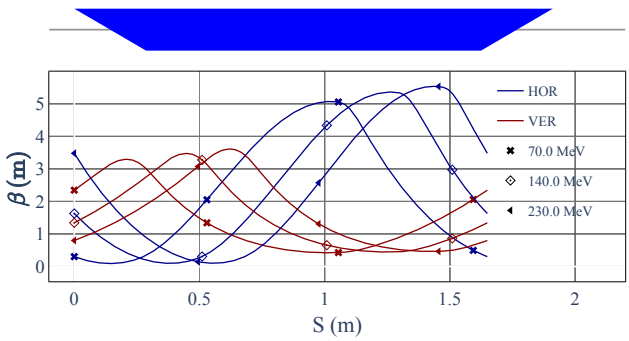

Figure 6: Evolution of the β-functions inside the FFA cell.

Based on the single cell periodic optics, we study the details of *block 2* (see Fig. 1). Stable trajectories are found for all energies. Figure 8a shows the results in a global coordinate system. The reduction of the trajectory-energy-excursion towards the isocenter is observed, a desired feature of the design. Fib. 8b details the trajectory excursions along the cell for different energies.

Figs. 9a and 9b represent the beam size in the horizontal and vertical planes for a beam energy of 140 MeV in the cell, assuming an emittance of 10 mm · mrad. In the first approximation, we compute the relation $\sigma = \sqrt{\beta\epsilon}$. We observe that the beam size in both planes has the same order

ISBN: 978-3-95450-227-1 ISSN: 2673-5490 doi:10.18429/JACoW-IPAC2022-THPOMS004

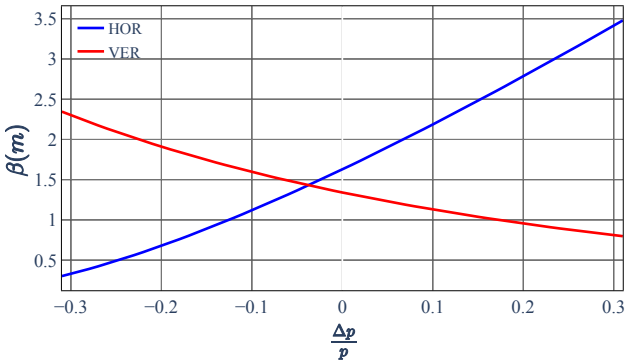

Figure 7: Initial β at the entrance of the cell as a function of the momentum deviation.

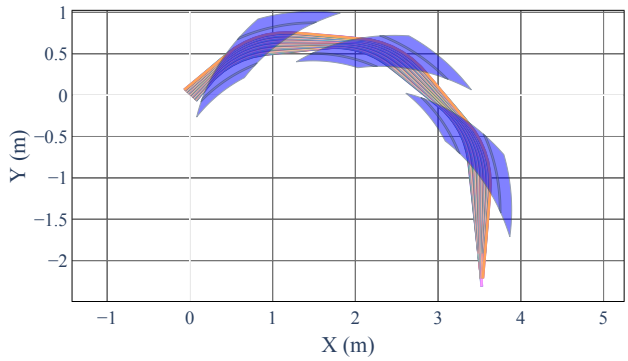

(a) In a global reference frame

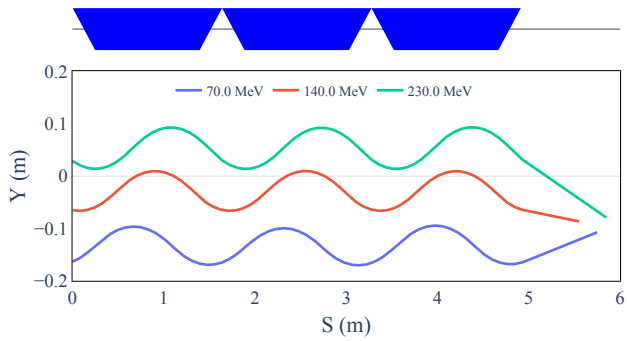

(b) In the Frenet-Serret reference frame

Figure 8: Tracking of particles along three FFAs cells. We observe a focusing of the different energies at the isocenter. By construction, the orbits are stable in the cells.

of magnitude and does not exceed 8 mm across the three cells. The scanning system will be designed to make the beam size as small as possible at the isocenter.

CONCLUSION

This paper has illustrated that RACCAM-based cells can be used to design an achromatic gantry for bending the beam towards the isocenter. These cells have the advantage of providing an achromatic beam transport across the entire energy range. By modifying the original cell design, we have reduced the radius of curvature to make the system as compact

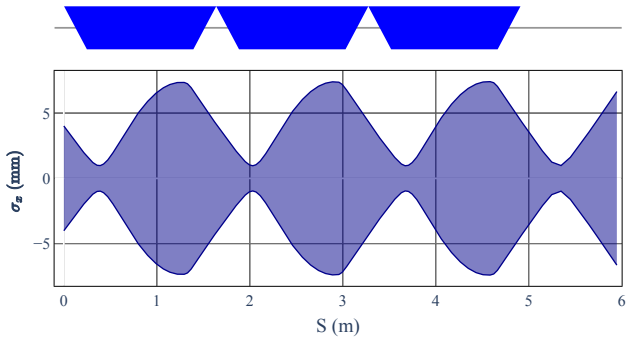

(a) Horizontal plane.

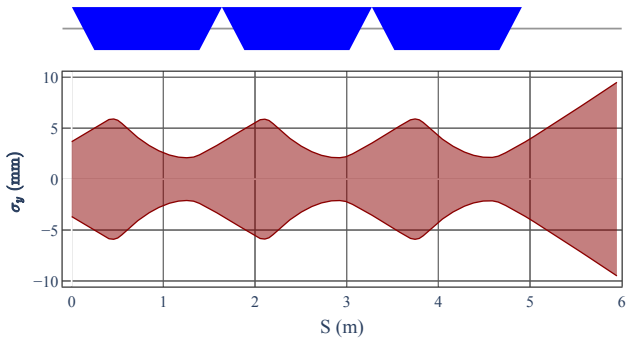

(b) Vorizontal plane.

Figure 9: Beam size along the line in the horizontal (9a) and vertical (9b) plane for an beam energy of 140 MeV and assuming an emittance of 10 mm·mrad. The beam size across the three cells doesn't exceed 8 mm in both planes.

as possible. The first studies have shown encouraging results, especially concerning the orbit excursion, which has been reduced from 66 to below 20 cm which is suitable for the scanning magnets. Moreover, we verified that the maximum field in the FFAs cells is below 2.3 T which guarantees that all the magnets remain normal-conducting. At the exit of three cells, we have shown that all energies are focused at the isocenter, which simplifies the scanning magnets' design. The next step of this project will focus on a detailed study of the beam size along the line, mainly by changing the emittance with the energy.

ACKNOWLEDGMENTS

This work has received funding from the Walloon Region (SPW-EER, Belgium) Win^{2}Wal program under grant agreement No. 1810110. The authors thank IBA for the support given to this work.

REFERENCES

[1] L. Toussaint *et al.*, "Towards proton arc therapy: physical and biologically equivalent doses with increasing number of beams in pediatric brain irradiation", *Acta Oncol.*, vol. 58, no. 10, 2019. doi:10.1080/0284186x.2019.1639823

ISBN: 978-3-95450-227-1 ISSN: 2673-5490 doi:10.18429/JACoW-IPAC2022-THPOMS004

[2] X. Li *et al.*, "The first prototype of spot-scanning proton arc treatment delivery", *Radiother. Oncol.*, vol. 137, pp. 130-136, 2019. doi:10.1016/j.radonc.2019.04.032

[3] J. R. Hughes and J. L. Parsons, "FLASH Radiotherapy: Current Knowledge and Future Insights Using Proton-Beam Therapy", *Int. J. Mol. Sci.*, vol. 21, no. 18, p. 6492, 2020. doi:10.3390/ijms21186492

[4] C. Hernalsteens *et al.*, "A novel approach to seamless simulations of compact hadron therapy systems for self-consistent evaluation of dosimetric and radiation protection quantities", *Europhys Lett*, vol. 132, no. 5, p. 50004, 2020. doi:10.1209/0295-5075/132/50004

[5] V. Derenchuk, "The ProNova SC360 Gantry, in: Modern Hadron Therapy Gantry Developments", Cockcroft Institute, Daresbury, UK, Tech. Rep., 2014.

[6] J. Fourrier *et al.*, "Spiral FFAG lattice design tools. Application to 6-D tracking in a proton-therapy class lattice", *Nucl. Instrum. Methods Phys. Res., Sect. A*, vol. 589, no. 2, pp. 133-142, 2008. doi:10.1016/j.nima.2008.01.082

[7] F. Méot, "RACCAM: An Example of Spiral Sector Scaling FFA Technology", Brookhaven National Laboratory, USA, Tech. Rep. BNL–211536-2019-NEWS, 2019. doi:10.2172/1507116

[8] S. Antoine *et al.*, "Principle design of a protontherapy, rapid-cycling, variable energy spiral FFAG", *Nucl. Instrum. Methods Phys. Res., Sect. A*, vol. 602, no. 2, pp. 293-305, 2009. doi:10.1016/j.nima.2009.01.025

[9] T. Planche *et al.*, "Design of a prototype gap shaping spiral dipole for a variable energy proton therapy FFAG", *Nucl. Instrum. Methods Phys. Res., Sect. A*, vol. 604, no. 3, pp. 435-442, 2009. doi:10.1016/j.nima.2009.02.026

[10] F. Méot, "The Ray-Tracing Code Zgoubi – Status", *Nucl. Instrum. Methods Phys. Res., Sect. A*, vol. 767, pp. 112-125, 2014. doi:10.1016/j.nima.2014.07.022

[11] F. Méot, "The Ray-Tracing Code Zgoubi", *Nucl. Instrum. Methods Phys. Res., Sect. A*, vol. 427, pp. 353–356, 1999. doi:10.1016/S0168-9002(98)01508-3

[12] C. Hernalsteens, R. Tesse, and M. Vanwelde, "Zgoubidoo", 2022. https://ulb-metronu.github.io/zgoubidoo/

[13] M. Vanwelde, E. Gnacadja, N. Pauly, E. Ramoisiaux, R. Tesse, and C. Hernalsteens, "The Zgoubidoo Python Framework for Ray-Tracing Simulations with Zgoubi: Applications to Fixed-Field Accelerators", presented at the IPAC'22, Bangkok, Thailand, Jun. 2022, paper MOPOST027, this conference.